Achieving Fast Reconnection in Resistive MHD Models via Turbulent Means

Giovanni Lapenta¹ and A. Lazarian²

Manuscript prepared for Nonlin. Processes Geophys.

¹Centrum voor Plasma-Astrofysica, Departement Wiskunde, Katholieke Universiteit Leuven, Celestijnenlaan 200B, 3001 Leuven, Belgium (EU)

Abstract. Astrophysical fluids are generally turbulent and this preexisting turbulence must be taken into account for the models of magnetic reconnection which are attepmted to be applied to astrophysical, solar or heliospheric environments. In addition, reconnection itself induces turbulence which provides an important feedback on the reconnection process. In this paper we discuss both theoretical model and numerical evidence that magnetic reconnection gets fast in the approximation of resistive MHD. We consider the relation between the Lazarian & Vishniac turbulent reconnection theory and Lapenta's numerical experiments testifying of the spontaneous onset of turbulent reconnection in systems which are initially laminar.

Keywords. Reconnection, Turbulence

1 Introduction

Astrophysical plasmas are known to be magnetized and turbulent. Magnetization of these fluids most frequently arises from the dynamo action to which turbulence is an essential component (see Schekochihin et al. 2007). The drivers of turbulence, e.g. supernovae explosions in the interstellar medium, inject energy at large scales and then the energy cascades down to small scales through a hierarchy of eddies spanning up over the entire inertial range. The famous Kolmogorov picture (Kolmogorov 1941) corresponds to hydrodynamic turbulence, but, as we discuss further, a qualitatively similar turbulence also develops in magnetized fluids/plasmas. The definitive confirmation of turbulence presence comes from observations, e.g. observations of electron density fluctuations in the interstellar medium, which produce a so-called Big Power Law in the Sky (Armstrong et al. 1994, Chepurnov & Lazarian 2010), with the spectral index

Correspondence to: Giovanni Lapenta (giovanni.lapenta@wis.kuleuven.be)

coinciding with the Kolmogorov one. A more direct piece of evidence comes from the observations of spectral lines. Apart from showing non-thermal Doppler broadening, they also reveal spectra of supersonic turbulent velocity fluctuations when analyzed with techniques like Velocity Channel Analysis (VCA) of Velocity Coordinate Spectrum (VCS) developed (see Lazarian & Pogosyan 2000, 2004, 2006, 2008) and applied to the observational data (see Padoan et al. 2004, 2009, Chepurnov et al. 2010) rather recently.

Reconnection is a process of changing magnetic flux topology and this process has been a challenge to understand in highly conductive astrophysical fluids. Naturally, it is important to understand the process of magnetic reconnection in reallistically turbulent state of the fluid. Observationally, it is also known that a high level of turbulence is present as outcome of solar flares, which are generally believed to be driven by magnetic reconnection. Therefore it is important to understand the mutual feedback of turbulence and reconnection and provide the connection between the existing theory, observations and numerical experiments. This is the goal of the present paper.

We consider both the model of turbulent reconnection suggested in Lazarian & Vishniac (1999, henceforth LV99) and numerical evidence of fast reconnection in a few numerical papers by Lapenta and coauthors. We search for the relation of the theory and observations.

The very idea that turbulence can influence magnetic reconnection is not new. However, LV99 model is radically different from its predecessors which also appealed to the effects of turbulence. For instance, unlike Speiser (1970) and Jacobson (1984) the model does not appeal to changes of the microscopic properties of the plasma. The nearest progenitor to LV99 was the work of Matthaeus & Lamkin (1985, 1986, henceforth ML), who suggested that magnetic reconnection may be fast due to a number of turbulence effects, e.g. multiple X points and turbulent EMF. However, ML did not realize

²Department of Astronomy, University of Wisconsin-Madison, 475 Charter St., USA

the key role of played by magnetic field-line wandering¹, and did not obtain a quantitative prediction for the reconnection rate, as did LV99. From the numerical simulations in ML obtaining the actual reconnection rate is not straightforward. They do not discuss the onset of reconnection from the laminar case, either. On the contrary, we shall demonstrate the results of simulations where both of these effects are studied and quantified.

In what follows, we discuss magnetic reconnection in turbulent fluid in §2, provide the numerical confirmations of the predictions of the LV99 model in §3, consider the spontaneous onset of reconnection in MHD simulations in §4 and the role of flow pattern in §5. We discuss the implications of the expected flares of reconnection in §6 and provide our summary in §7.

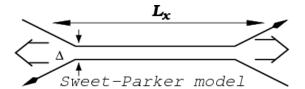
2 Reconnection can be Fast in Turbulent Plasmas

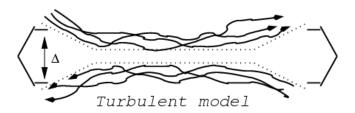
Astrophysical plasmas are often highly ionized and highly magnetized (Parker 1970). The evolution of the magnetic field in a highly conducting fluid can be described by a simple version of the induction equation

$$\frac{\partial \mathbf{B}}{\partial t} = \nabla \times (\mathbf{v} \times \mathbf{B} - \eta \nabla \times \mathbf{B}), \tag{1}$$

where B is the magnetic field, v is the velocity field, and η is the resistivity coefficient. Under most circumstances this is adequate for discussing the evolution of magnetic field in an astrophysical plasma. When the dissipative term on the right hand side is small, as is implied by simple dimensional estimates, the magnetic flux through any fluid element is constant in time and the field topology is an invariant of motion. On the other hand, reconnection is observed in the solar corona and chromosphere (Innes et al. 1997, Yokoyama & Shibata 1995, Masuda et al. 1994, Ciaravella & Raymond 2008), its presence is required to explain dynamo action in stars and galactic disks (Parker 1970, 1993), and the violent relaxation of magnetic fields following a change in topology is a prime candidate for the acceleration of high energy particles (de Gouveia Dal Pino & Lazarian 2003, henceforth GL03, 2005, Lazarian 2005, Drake et al. 2006, Lazarian & Opher 2009, Drake et al. 2010) in the universe. Quantitative general estimates for the speed of reconnection start with two adjacent volumes with different large scale magnetic field directions (Sweet 1958, Parker 1957).

LV99 we introduced a model that included the effects of magnetic field line wandering (see Figure 1). The model relies on the nature of three-dimensional magnetic field wandering in turbulence. This nature is different in three and two dimensions, which provides the major difference between the LV99 model and the earlier attempts to solve the problem of magnetic reconnection appealing to turbulence (Matthaeus





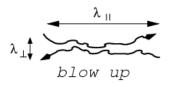


Fig. 1. Upper plot: Sweet-Parker model of reconnection. The outflow is limited by a thin slot Δ , which is determined by Ohmic diffusivity. The other scale is an astrophysical scale $L\gg\Delta$. Middle plot: Reconnection of weakly stochastic magnetic field according to LV99. The model that accounts for the stochasticity of magnetic field lines. The outflow is limited by the diffusion of magnetic field lines, which depends on field line stochasticity. Low plot: An individual small scale reconnection region. The reconnection over small patches of magnetic field determines the local reconnection rate. The global reconnection rate is substantially larger as many independent patches come together. From Lazarian et al. 2004.

& Lamkin 1985). The effects of compressibility and heating which were thought to be important in the earlier studies (Matthaeus & Lamkin 1985, 1986) do not play the role for the LV99 model either. The model is applicable to any weakly perturbed magnetized fluid, irrespectively, of the degree of plasma being collisional or collisionless (cf. Shay et al. 1998).

Two effects are the most important for understanding of the nature of reconnection in LV99. First of all, in three dimensions bundles of magnetic field lines can enter the reconnection region and reconnection there independently (see Figure 1), which is in contrast to two dimensional picture where in Sweet-Parker reconnection the process is artificially constrained. Then, the nature of magnetic field stochasticity and therefore magnetic field wandering (which determines the outflow thickness, as illustrated in Figure 1) is very different in 2D and the real 3D world (LV99). In other words, removing artificial constraints on the dimensionality of the reconnection region and the magnetic field being absolutely

¹Instead a discussion other effects, like heating, was presented. Those do not play a role in LV99.

straight, LV99 explores the real-world astrophysical reconnection

Our calculations in LV99 showed that the resulting reconnection rate is limited only by the width of the outflow region. This proposal, called "stochastic reconnection", leads to reconnection speeds close to the turbulent velocity in the fluid. More precisely, assuming isotropically driven turbulence characterized by an injection scale, l, smaller than the current sheet length, we find

$$V_{rec} \approx \frac{u_l^2}{V_A} (l/L)^{1/2} \approx u_{turb} (l/L)^{1/2},$$
 (2)

where u_l is the velocity at the driving scale and u_{turb} is the velocity of the largest eddies of the strong turbulent cascade. Note, that here "strong" means only that the eddies decay through nonlinear interactions in an eddy turn over time (see more discussion of the LV99). All the motions are weak in the sense that the magnetic field lines are only weakly perturbed.

It is useful to rewrite this in terms of the power injection rate P. As the perturbations on the injection scale of turbulence are assumed to have velocities $u_l < V_A$, the turbulence is weak at large scales. Therefore, the relation between the power and the injection velocities are different from the usual Kolmogorov estimate, namely, in the case of the weak turbulence $P \sim u_l^4/(lV_A)$ (LV99). Thus we get,

$$V_{rec} \approx \left(\frac{P}{LV_A}\right)^{1/2} l,$$
 (3)

where l is the length of the turbulent eddies parallel to the large scale magnetic field lines as well as the injection scale.

The reconnection velocity given by equation (3) is obtained in MHD limit and therefore it does not depend on resistivity or plasma effects. Therefore LV99 model predicts that for sufficiently high level of turbulence collisionless and collisional fluids should reconnect at the same rate.

3 Fast reconnection in Turbulent MHD Simulations

Here we describe the results of a series of three dimensional numerical simulations aimed at adding turbulence to the simplest reconnection scenario and testing equation (3). We take two regions with strongly differing magnetic fields lying next to one another. The simulations are periodic in the direction of the shared field (the z axis) and are open in the reversed direction (the x axis). The external gas pressure is uniform and the magnetic fields at the top and bottom of the box are taken to be the specified external fields plus small perturbations to allow for outgoing waves. The grid size in the simulations varied from 256x512x256 to 512x1028x512 so that the top and bottom of the box are far away from the current sheet and the region of driven turbulence around it. At the sides of the box where outflow is expected the derivatives of the dynamical variables are set to zero. A complete description

of the numerical methodology can be found in Kowal et al. (2009). All our simulations are allowed to evolve for seven Alfven crossing times without turbulent forcing. During this time they develop the expected Sweet-Parker current sheet configuration with slow reconnection. Subsequently we turn on isotropic turbulent forcing inside a volume centered in the midplane (in the xz plane) of the simulation box and extending outwards by a quarter of the box size. The turbulence reaches its full amplitude around eight crossing times and is stationary thereafter.

In Figure 2 we see the current density on an xy slice of the computational box once the turbulence is well developed. As expected, we see that the narrow stationary current sheet characteristic of Sweet-Parker reconnection is replaced by a chaotic structure, with numerous narrow peaks in the current density. Clearly the presence of turbulence has a dramatic impact on the structure of the reconnection zone. In addition, we see numerous faint features indicating weak reconnection between adjacent turbulent eddies.

The speed of reconnection in three dimensions can be hard to define without explicit evaluation of the magnetic field topology. However, in this simple case we can define it as the rate at which the x component of the magnetic field disappears. More precisely, we consider a yz slice of the simulation, passing through the center of the box. The rate of change of the area integral of $-B_x$ — is its flux across the boundaries of the box minus the rate at which flux is annihilated through reconnection (see more discussion in Kowal et al. 2009)

$$\partial_t \left(\int |B_x| dz dy \right) = \oint sign(B_x) vec E d \pmb{l} - 2 V_{rec} B_{x,ext} L_z(\textbf{4})$$

where electric field is $E = v \times B - \eta j$, $B_{x,ext}$ is the absolute value of B_x far from the current sheet and L_z is the width of the box in the z direction. This follows from the induction equation under the assumption that the turbulence is weak to lead to local field reversals and that the stresses at the boundaries are weak to produce significant field bending there. In other words, fields in the x direction are advected through the top and bottom of the box, and disappear only through reconnection. Since we have assumed periodic boundary conditions in the z direction the boundary integral on the right hand side is only taken over the top and bottom of the box. By design this definition includes contributions to the reconnection speed from contracting loops, where Ohmic reconnection has occurred elsewhere in the box and $|B_x|$ decreases as the end of a reconnected loop is pulled through the plane of integration. It is worth noting that this estimate is roughly consistent with simply measuring the average influx of magnetic field lines through the top and bottom of the computational box and equating the mean inflow velocity with the reconnection speed. Following equation (4) we can evaluate the reconnection speed for varying strengths and scales of turbulence and varying resistivity.

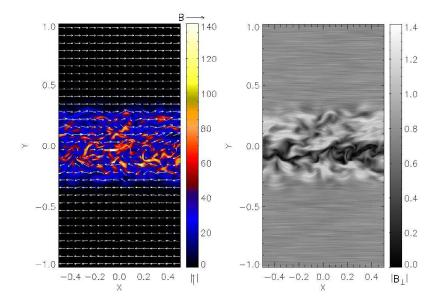


Fig. 2. Left panel: Current intensity and magnetic field configuration during stochastic reconnection. We show a slice through the middle of the computational box in the xy plane after twelve dynamical times for a typical run. The shared component of the field is perpendicular to the page. The intensity and direction of the magnetic field is represented by the length and direction of the arrows. The color bar gives the intensity of the current. The reversal in B_x is confined to the vicinity of y=0 but the current sheet is strongly disordered with features that extend far from the zone of reversal. Right panel: Representation of the magnetic field in the reconnection zone with textures.

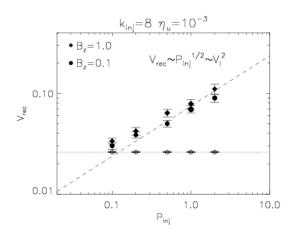


Fig. 3. Reconnection speed versus input power for the driven turbulence. We show the reconnection speed, defined by equation (4) plotted against the input power for an injection wavenumber equal to 8 (i.e. a wavelength equal to one eighth of the box size) and a resistivity ν_u . The dashed line is a fit to the predicted dependence of $P^{1/2}$ (see eq. (3)). The horizontal line shows the laminar reconnection rates for each of the simulations before the turbulent forcing started. Here the uncertainty in the time averages are indicated by the size of the symbols and the variances are shown by the error bars.

In Figure 3 we see the results for varying amounts of input power, for fixed resistivity and injection scale as well as for the case of no turbulence at all. The line drawn through the simulation points is for the predicted scaling with the square root of the input power. The agreement between equation (3) and Figure 3 is encouraging but does not address the most important aspect of stochastic reconnection, i.e. its insensitivity to η .

In Figure 4 we plot the results for fixed input power and scale, while varying the background resistivity. In this case η is taken to be uniform, except near the edges of the computational grid where it falls to zero over five grid points. This was done to eliminate edge effects for large values of the resistivity. We see from the Figure 4 that the points for laminar reconnection scale as $\sqrt{\eta}$, the expected scaling for Sweet-Parker reconnection. In contrast, the points for reconnection in a turbulent medium do not depend on the resistivity at all. In summary, we have tested the model of stochastic reconnection in a simple geometry meant to approximate the circumstances of generic magnetic reconnection in the universe. Our results are consistent with the mechanism described by LV99. The implication is that turbulent fluids in the universe including the interstellar medium, the convection zones of stars, and accretion disks, have reconnection speeds close to the local turbulent velocity, regardless of the local value of resistivity. Magnetic fields in turbulent fluids can change their topology on a dynamical time scale.

In Kowal et al. (2009) we also studied the dependence of the reconnection on the anomalous resistivity, which in-

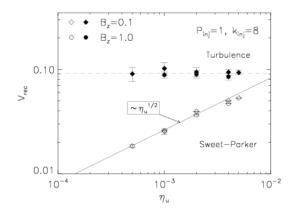


Fig. 4. Reconnection speed versus resistivity. We show the reconnection speed plotted against the uniform resistivity of the simulation for an injection wavenumber of 8 and an injected power of one. We include both the laminar reconnection speeds, using the hollow symbols, fit to the expected dependence of η_u , and the stochastic reconnection speeds, using the filled symbols. As before the symbol sizes indicate the uncertainty in the average reconnection speeds and the error bars indicate the variance. We included simulations with large, $B_z=1$, and small, $B_z=0.1$, guide fields.

creases effective resistivity for high current densities. The anomalous resistivity can be used as a proxy for plasma effects, e.g. collisionless effects in reconnection. While it enhances the local speed of individual reconnection events results in Kowal et al. (2009) testify that the total reconnection rate does not change. In addition, the study of numerical effects is presented in Lazarian et al. (2011). Numerical resistivity decreases with increase of the numerical resolution. Therefore, if the numerical effects were influencing the reconnection rate, the increase of the resolution would decrease the reconnection rates. This is not what is seen in simulations (Lazarian et al. 2011). If anything, the reconnection rates slightly increase with the increase of resolution which is due to the fact that the turbulence proceeds to smaller scales. As a result, field wandering over smaller scales is available and therefore the outflow region gets slightly thicker as the numerical viscosity decreases.

Finally, it is important to give a few words in relation to our turbulence driving. We drive our turbulence solenoidally to minimize the effects of compression, which does not play a role in LV99 model. The turbulence driven in the volume around the reconnection layer corresponds to the case of astrophysical turbulence, which is also volume-driven. On the contrary, the case of the turbulence driven at the box boundaries would produce spatially inhomogeneous imbalanced turbulence for which we do not have analytical predictions (see discussion of such turbulence in Beresnyak & Lazarian 2009). We stress, that it is not the shear size of our numerical simulations, but the correspondence of the observed scalings to those predicted in LV99 that allows us to claim that we

proved that the 3D reconnection is fast in the presence of turbulence.

4 Spontaneous onset of Turbulent Reconnection in Laminar System

Macroscopically laminar systems can spontaneously transition toward unsteady regimes characterised by faster rates and presenting features that are closely related to the turbulent reconnection regimes described above.

The long recognized natural pathway for reconnection in laminar systems is the Sweet-Parker (SP) regime (Sweet, 1958; Parker, 1963). In SP reconnection a thin and elongated current layer forms separating two areas of opposing magnetic polarity. The plasma and the field flows towards the current layer in the direction normal to the elongated side and outflows along the axis of the current. Figure 5-a shows the typical flow pattern.

The SP current layer, like any other current layer, is in itself unstable to the tearing mode (Biskamp, 1993, 2000) producing secondary islands. The presence of the flow pattern and the finite length of the layer prevent a direct application of the textbook analysis of the tearing mode. The first studies of the instability of SP layers were reported by Bulanov et al. (1979) and are summarised in recent textbooks (Biskamp, 1993, 2000). The conclusion was that for aspect ratios of the SP layer (length of the current channel, Δ over its width δ) exceeding approximately 100, the SP layer becomes unstable. The aspect ratio of a SP layer is directly determined by the resistivity in the system. Using the parametrization of the resistivity with the Lundquist number S, the aspect ratio is simply $\Delta/\delta = \sqrt{S}$ (Priest and Forbes, 2000). It follows that given a sufficiently low resistivity, corresponding to a Lundquist number in excess of $S = 10^4$, a SP will become naturally unstable to formation of secondary islands.

Low resistivity was not easily accessible to simulations until recently. At low resolutions, the numerical resistivity exceeds the intended low resistivity preventing the exploration of truly low resistive regimes. However, in recent years truly low resistivity regimes became accessible thanks to modern numerical methods and state of the art computational facilities. Great progress has been made in understanding this spontaneous transition from laminar SP reconnection to an unsteady regime characterised by a random onset of secondary islands.

The configuration of a SP layer is intrinsically 2D and requires a 2D analysis (Ni et al., 2010). Furthermore the SP layer is embedded in macroscopic configurations that further affect the stability and evolution (Schindler and Birn, 1999). However, a reduced 1D analysis (Loureiro et al., 2007) can still take into account the effects of the flow present in the SP layer. The flow has a stabilising effect (Bulanov et al., 1978) that prevents the onset for aspect ratios below approximately 100, but at higher aspect ratios (corresponding to

higher Lundquist numbers) the instability is present. The growth rate of the secondary instability is found to scale as $\gamma \approx S^{1/4}$ and the fastest growing mode corresponds to a number of islands that scales as $S^{3/8}$ (Huang and Bhattacharjee, 2010). The power is positive: the growth rate of the secondary instability is faster for lower resistivity. Additionally as the resistivity is lowered and the aspect ratio is increased, the number of magnetic islands increases. The emerging picture from linear theory is then clear: as the Lundquist number is increased the SP layer becomes progressively more elongated, with a higher aspect ratio. The more elongated the SP layer becomes, the larger the number of secondary islands becomes, and the faster they grow after forming. A clear indication of transition towards a turbulent regime like that covered in the previous sections.

The prediction of the linear theory with respect to the number and growth rate of secondary islands have been tested and verified in carefully designed simulations (Samtaney et al., 2009; Cassak et al., 2009; Bhattacharjee et al., 2009).

Similarly, the threshold for onset (S approximately 10⁴) has been also confirmed (Skender and Lapenta, 2010). Additionally, the simulation studies have proven that turbulence, if present, has a direct impact on the process. The presence of pre-existing fluid turbulence changes the onset of the secondary island instability (Skender and Lapenta, 2010; Loureiro et al., 2009). A SP layer still forms also in presence of moderate levels of turbulence but it is more prone to become unstable. The stronger seed reduces the threshold for the onset and the system transitions more quickly to an unsteady regime of reconnection characterized by multiple islands and reconnection sites. Indeed in all simulations the instability of the SP layer is seeded by numerical noise. Spectral methods avoid such noise completely and inedeed the instability cannot develop (Ng and Ragunathan, 2011), unless a seed in the form of a low level of turbulence is added explicitly.

An important consequence of the formation of secondary islands and the onset of unsteady reconnection is the acceleration of the reconnection process (Lapenta, 2008). Reconnection is usually defined as fast when two conditions are met.

First, the reconnection rate should be independent of the mechanism that allows the decoupling of the plasma (and specifically the electrons in the case of advanced two fluid and kinetic models). In resistive MHD, the mechanisms allowing such decoupling are resistivity and, possibly, viscosity. With the onset of secondary islands, simulations observe not only an increased rate of reconnection but careful studies varying the resistivity in the system have shown that the rate becomes insensitive or even independent of resistivity altogether (Lapenta, 2008; Loureiro et al., 2009; Huang and Bhattacharjee, 2010; Uzdensky et al., 2010).

Second, for reconnection to be fast in absolute terms, its rate must be a significant fraction of the local Alfvén speed measured with the density and magnetic field strength at the entry of the reconnection region $v_{A,in}$. For a reconnecting Harris sheet, Skender and Lapenta (2010) report a rate of approximately $\Delta \dot{\Psi}/v_{A,in}B_{in} \approx .015$ with peaks of twice that value. Note that the value reported by Skender and Lapenta (2010) is computed with a different normalisation Alfvén speed based on the peak rather than the inflow density that is a factor of 10 smaller. Here we prefer to translate the result in terms of to the actual Alfvèn speed of the inflowing plasma for better comparison with the other litarature. For force free equlibria, the peak reconnection rate also nearly reaches $\Delta \Psi / v_{A,in} B_{in} \approx .015$ (Skender and Lapenta, 2010). Similarly, in the case of the reconnection induced by the coalescence of two magnetic islands, Huang and Bhattacharjee (2010) report a reconnection rate of $\Delta \Psi / v_A B_0 \approx .01$, in agreement with the case of the Harris sheet. The reconnection rate of unsteady MHD resistivity is therefore somewhat lower than that typical of the fastest kinetic regimes (peak rate of $\Delta\Psi/v_{A,in}B_{in}\approx .1$ (Birn and et al., 2001)) but is still very strong.

Many of the properties of the fast reconnection process following the onset of the secondary islands instability can be understood with a simplified approach based on the properties of the tearing mode (Bhattacharjee et al., 2009). For an initial current sheet with a magnetic field profile

$$\mathbf{B}(z) = B_0 \tanh(z/a)\hat{\mathbf{x}} \tag{5}$$

the linear theory based on reduced MHD with uniform resistivity η predicts a maximum growth rate (Schindler, 2006, p.242):

$$\gamma_{max} a / v_A = 0.623 \cdot (\mu_0 a v_A / \eta)^{-1/2} \tag{6}$$

corresonding to the wave number:

$$k_{max}a = 1.358 \cdot (\mu_0 a v_A/\eta)^{-1/4}$$
 (7)

In the case of the stability of a SP layer, one can simply use the same result but consider that the initial state is itself the SP layer, with a thickness that is proportional to the square of the resistivity, $a=\eta^{1/2}$. It immediately follows that the fastest growing mode of the secondary island instability scales as $k \propto \eta^{-3/8}$ and the corresponding growth rate as $\gamma \propto \eta^{-1/4}$. These simple estimates agree remarkably with the more in depth analysis by Loureiro et al. (2007).

The argument can be carried further in the non-linear regime to estimate the non-linear reconnection rate during the subsequent growth of the islands. In the case of the tearing mode, the island growth is governed by the Rutherford equation (Rutherford, 1973), stating that the size of the magnetic islands (w_I) grows in time linearly (rather than exponentially). The temporal derivative of the size of a magnetic island is $\dot{w_I} \propto \eta \Delta'/\mu_0$ (Kadomtsev, 1992, p. 76), where, for the initial configuration assumed above,

$$\Delta' = \frac{2}{a} \left(\frac{1}{ka} - ka \right) \tag{8}$$

At long wavelengths, where ka << 1, $\Delta' \propto a^{-2}$, and assuming again the initial thickness to be that of the SP layer, the Rutherford equation leads to a rate of island growth independent of resistivity, $\dot{w_I} \propto \eta^0$.

Note that the dependence on k is not considered in the scaling argument because the secondary islands are observed in the simulation to coalesce and the value of k is expected to settle on a value constrained more by the macroscopic system rather than by the fastest growing linear mode.

5 Role of the flow pattern in unsteady reconnection

A consequence of the onset of the secondary island instability is the profound modification of the plasma flow patterns in the reconnection region. To investigate the flow, a specific simulation is used. The initial state is a Harris sheet with magnetic field given by eq. (5), uniform initial temperature corresponding to $v_s/v_A=1$ and density

$$\rho = \rho_0 / \cosh^2(z/a) + \rho_b \tag{9}$$

with $\rho_b = \rho_0/10$. The evolution is followed with viscoresistive MHD, using the FLIP3D-MHD code (Brackbill, 1991).

The simulations have uniform resistivity corresponding to a Lundquist number, $S=\eta_0 a v_A/\eta=10^4$ and a viscosity corresponding to a Reynolds number, $R=\rho_0 v_A a/\eta=10^4$. All results are presented in normalised units where the magnetic field is normalised to B_0 , the density to ρ_0 , time with the Alfvén time $\tau_A=a/v_A$, space with the initial current sheet thickness a and velocity with the Alfvén speed $v_A=B_0/(\mu_0\rho_0)^{1/2}$. The simulation box has sides $L_x/a=240$ and $L_z=60$. The code is 3D but the y dependence is suppressed.

During the SP regime, the flow is primarily directed normal to the sides of the SP layer. In the two inflow sides, the flow is vertical, and in the two outflow sides it becomes horizontal, veering within the SP layer. Figure 5-a shows such a configuration for the present simulation. The actual flow in the simulation is just as the typical textbook SP cartoon (Biskamp, 2000).

As the simulation evolves, the flow pattern changes and becomes primarily focused near the separatrices. This is a typical feature of the flow in presence of magnetic islands due to the tearing instability. Figure 5-b and Fig. 5-c demonstrate the transition. A x-point is forming in the center as a consequence of the secondary island instability. The flow pattern becomes now just like the textbook cartoon of the flow near an x-point in the tearing mode (Biskamp, 2000).

Still later times are shown in Fig. 6. After the onset of the secondary island instability progressively more secondary islands and x-points are formed. The new formed islands coalesce with pre-existing islands and migrate with the flow towards the two ends of the simulation box (Lapenta, 2008). The present simulation uses periodic boundary conditions

but the same series of events develops also with open boundary conditions (Skender and Lapenta, 2010; Bettarini and Lapenta, 2010) with the only difference that the flow carries the formed islands outside the open boundaries.

The presence of multiple islands causes the flow to form characteristics loops. In a previous paper (Lapenta, 2008), the name conveyor belts was used to explain the role of such flow loops. The flow assumes a pattern where the flow lines that come out of the reconnection process bend and return towards the same reconnection region. The effect is similar to that of recursive reconnection (Parnell et al., 2008) observed in magnetic skeleton configurations representative of solar coronal configurations. In recursive reconnection the outflow of one reconnection site feeds into another. In the present simulation the same recursive process is also observed. In Fig 6-c the outflow from the x-point located at x/a = 115 feeds the reconnection process at the x-point located at x/a = 90 (and the similarly by symmetry on the other side). But more conspicuously, the same reconnection x-point at x/a = 115 feeds itself with most flow lines going out of it and coming back forming a conveyor belt.

In accordance with the theoretical predictions above for reconnection to be fast the flow must become stronger in the unsteady regime. Comparing the scales in Fig. 5 with Fig. 6, the flow accelerates strongly. Figure 7 shows separately the inflow component along z and the outflow component along x. The outflow is at the Alfvén speed and the inflow is a significant fraction of it. At steady state the inflow speed equals the reconnection electric field and is by definition the reconnection rate.

The concept of streamlines and in particular of conveyor belts should not be confused with actual recirculation of plasma. The flow pattern is distinct from the matter actually flowing. On those stepping into rivers staying the same other and other waters flow (Heraclitus of Ephesus, 2001, DK22B12,Fragment 91). The flow can present the same pattern over a certain period but the plasma elements going through the flow are other and other. The streamlines are instant photos of the velocity field at a given instant. They are obtained here with the paraview software using the fourthfifth order Runge-Kutta ODE solver that traces the lines everywhere tangent to the velocity field at that instant. But an actual fluid element feels at every instant the local speed at that instant. A moment later it feels another speed. Flow lines are not the same thing as particle trajectories. To analyse actual trajectories of fluid elements we use Lagrangian markers. Lagrangian markers are real particles of the fluid that move with the local instantaneous velocity just as a physical fluid would. These are not kinetic particles moving with their peculiar speed but rather fluid elements moving with the local flow speed. The FLIP3D-MHD code is based on a dual grid-particle representation that includes the presence of Lagrangian markers (Brackbill, 1991).

Figure 8 shows a selected number of trajectories of Lagrangian markers. The initial starting point at time t=0

in the simulation is chosen appropriately to identify particles that will go through multiple reconnection sites. Some trajectories only pass reconnection once: those are particles that are drawn toward the neutral line (z/a = 30) and then ejected away from it (reddish trajectories on the left and light cyan on the right). However, there are other classes of trajectories (green on the left and magenta on the right) that are first drawn towards the neutral line and after being pushed away, come back a second time towards the neutral line and then are finally ejected away from it. These are particles that are captured in the conveyor belts and are pushed towards a reconnection site and then away from it and then towards another one again. Note, however, that these trajectories are still monotonic in the horizontal direction: the same particle does not turn back to go towards the same x-point. For example on the left of center, the markers first take part to reconnection at the site located near x/a = 115 and then at x/a = 90. No particle is detected to go through the same reconnection site twice. Just as the citation by Heraclitus suggested.

6 Discussion

A magnetic field embedded in a laminar perfectly conducting fluid preserves its topology for all time (Parker 79). Although ionized astrophysical objects, like stars and galactic disks, are almost perfectly conducting, they show indications of changes in topology, "magnetic reconnection", on dynamical time scales (Parker 1970, Lovelace 1976, Priest & Forbes 2002). Reconnection can be observed directly in the solar corona (Innes et al 1997, Yokoyama & Shibata 1995, Masuda et al. 1994), but can also be inferred from the existence of large scale dynamo activity inside stellar interiors (Parker 1993, Ossendrijver 2003). Solar flares (Sturrock 1966) and γ -ray busts (Fox et al. 2005, Galama et al. 1998) are usually associated with magnetic reconnection. Previous work has concentrated on showing how reconnection can be rapid in plasmas with very small collisional rates (Shay et al. 1998, Drake 2001, Drake et al. 2006, Daughton et al. 2006), which substantially constrains astrophysical applications of the corresponding reconnection models².

In comparison, our results point out to an attractive universal astrophysical solution for the magnetic reconnection: magnetic reconnection in presence of turbulence is always fast independently of the collisional or collisionless state of plasmas. The formal criterion of the applicability of the LV99

model based on the MHD approximation to realistic plasmas is discussed in Eyink, Lazarian & Vishniac (2011).

Our paper provides a connection between the LV99 theory and numerical simulations demonstrating the spontaneous onset of fast reconnection. Indeed, according the LV99 model the reconnection in the initially laminar state is slow. The outflow, however, incites turbulence in the system. This turbulence induces faster reconnection and a wider outflow gets more turbulent. This should induce a positive feedback process which results in the flare of reconnection. We believe that this is what is the actual theoretical explanation of the spontaneous onset of fast reconnection observed in papers by Lapenta et al.

The spontaneous onset of reconnection is likely to be the cause of the solar flares. The flares require the accumulation of magnetic flux of opposite polarity prior to the flare. The accumulation means low reconnection rate, which is readily achived for the observed mean level of turbulence in solar atmosphere (Eyink et al. 2011). As the flux is accumulated the effects that we described in this paper are expected to come into place and a abrupt release of energy through magnetic reconnection is expected. A similar process can take place during gamma ray busts (Lazarian et al. 2002, Zhang & Yan 2011). A relatively low level of turbulence is a prerequisit for the flares. In the presence of high amplitude turbulence, reconnection is going to be fast from the very beginning preventing the accumulation of magnetic flux at the pre-flare stage

Observationally, predictions of the LV99 model for flares are in rough agreement with the estimates of the thickness of the outflow regions obtained in observations (Ciravella & Raymond 2008). In addition, the initiation of the reconnection by Alfvenic perturbations predicted in LV99 was confirmed by observations in Sych et al. (2009). Direct observations of turbulent reconnection in other environments, e.g. in interstellar medium are not feasible at the moment. However, the indirect evidence of LV99-type reconnection comes from the observations of magnetic fields in molecular clouds and accretion disks. In fact, on the basis of LV99 model Lazarian (2005) predicted the process of magnetic field removal termed "reconnection diffusion". Numerical studies of the reconnection diffusion (see Santo de Lima et al. 2010, 2011) deliver results on expected magnetic flux diffusion that are consistent with observations.

The caveat here is that the LV99 model is the 3D model and it appeals to the 3D wondering of magnetic field lines. We believe that the fact that the acceleration was observed also in 2D systems testify that the modification of LV99 model is applicable to the systems of reduced dimentionality. It is discussed in Eyink et al. (2011) that the existence of the "rough" turbulent velocity field should induce the Richarson diffusion and therefore the effective magnetic field wandering. The corresponding theory have not been developed for the 2D turbulence. However, results on the acceleration of reconnection in the presence of turbulence (Loreiro ..., Kulpa-

² We note that if magnetic reconnection is slow in some astrophysical environments, this automatically means that the results of present day numerical simulations in which the reconnection is inevitably fast due to numerical diffusivity do not correctly represent magnetic field dynamics in these environments. If, for instance, the reconnection were slow in collisional media this would entail the conclusion that the entire crop of interstellar, protostellar and stellar MHD calculations would be astrophysically irrelevant.

Dubel et al. 2010) suggest that the results of LV99 may carry over to 2D systems. However, as turbulence in 2D and 3D is different, we feel that it does not worth rederiving the LV99 results for 2D, but it is better to concentrate on matching the quantitative results for the actual real world 3D reconnection as numerical simulations are getting sufficiently powerful to study the effects in 3D. This is the theme of our intended next paper.

Our paper sends a warning signal to a naive interpretation of astrophysical reconnection within laminar reconnection models. We showed that pre-existing turbulence as well as turbulence induced by the process of magnetic reconnection itself can dramatically change the reconnection rates. Interestingly enough, the small - scale reconnection events may be determined by small scale physics, but the total reconnection rates may still be determined by turbulent level in the system.

7 Summary

The results of the present paper can be briefly summarised in the following way:

- 1. The LV99 theory of fast turbulent reconnection and more recent results on the spontaneous onset of turbulent reconnection are related to each other. We claim that the flares of reconnection observed in simulations are due to the feedback by turbulence induced by the outflow on the reconnection process.
- 2. The numerical results suggest that flares of magnetic reconnection, e.g. explaining solar flares, may be explained on the basis of pure resistive MHD.
- 3. Our work testifies in favor of a widely applicable model of astrophysical reconnection that is independent of subtle plasma effects. At the same time it send a warning to attempts to model astrophysical reconnection without including effects of turbulence.

Acknowledgements. The research of AL is supported by the NSF grant AST 0808118 and the Center for Magnetic Self Organization in Laboratory and Astrophysical Plasmas (CMSO).

References

- Beck, R., Brandenburg, A., Moss, D., Shukurov, A., Sokoloff, D. 1996. Galactic Magnetism: Recent Developments and Perspectives. Annual Review of Astronomy and Astrophysics 34, 155– 206.
- Beresnyak, A., Lazarian, A. 2009. Structure of Stationary Strong Imbalanced Turbulence. The Astrophysical Journal 702, 460–471.
- Bettarini, L. and Lapenta, G.: Spontaneous non-steady magnetic reconnection within the solar environment, Astron. Astrophys., 518, A57+, doi:10.1051/0004-6361/200913652, 2010.

- Bhattacharjee, A., Huang, Y.-M., Yang, H., and Rogers, B.: Fast reconnection in high-Lundquist-number plasmas due to the plasmoid Instability, Physics of Plasmas, 16, 112 102—+, doi:10. 1063/1.3264103, 2009.
- Birn, J. and et al.: Geospace Environmental Modeling (GEM) magnetic reconnection challenge., J. Geophys. Res., 106, 3715–3719, 2001.
- Biskamp, D. 1986. Magnetic reconnection via current sheets. Physics of Fluids 29, 1520–1531.
- Biskamp, D.: Nonlinear Magnetohydrodynamics, Cambridge University Press, Cambridge, 1993.
- Biskamp, D.: Magnetic Reconnection in Plasmas, Cambridge University Press, Cambridge, 2000.
- Brackbill, J.: FLIP MHD: A particle-in-cell method for magneto-hydrodynamics, J. Comp. Phys., 96, 163, 1991.
- Brandenburg, A., Subramanian, K. 2005. Astrophysical magnetic fields and nonlinear dynamo theory. Physics Reports 417, 1–209.
- Bulanov, S. V., Syrovatskii, S. I., and Sakai, J.: Stabilizing influence of plasma flow on dissipative tearing instability, Soviet Journal of Experimental and Theoretical Physics Letters, 28, 177—+, 1978.
- Bulanov, S. V., Sakai, J., and Syrovatsii, S. I.: Tearing-mode instability in approximately steady MHD configurations, Sov. J. Plasma Phys., 5, 157, 1979.
- Cassak, P. A., Shay, M. A., and Drake, J. F.: Scaling of Sweet-Parker reconnection with secondary islands, Physics of Plasmas, 16, 120702—+, doi:10.1063/1.3274462, 2009.
- Chepurnov, A., Lazarian, A. 2010. Extending the Big Power Law in the Sky with Turbulence Spectra from Wisconsin H α Mapper Data. The Astrophysical Journal 710, 853–858.
- Ciaravella, A., Raymond, J. C. 2008. The Current Sheet Associated with the 2003 November 4 Coronal Mass Ejection: Density, Temperature, Thickness, and Line Width. The Astrophysical Journal 686, 1372–1382.
- Cummings, A. C., Stone, E. C. 1998. Anomalous Cosmic Rays and Solar Modulation. Space Science Reviews 83, 51–62.
- Daughton, W., Scudder, J., Karimabadi, H. 2006. Fully kinetic simulations of undriven magnetic reconnection with open boundary conditions. Physics of Plasmas 13, 072101.
- Daughton, W., Roytershteyn, V., Albright, B. J., Bowers, K., Yin, L., Karimabadi, H. 2008. Reconnection Dynamics in Semi-Collisional Plasmas. AGU Fall Meeting Abstracts A1705.
- de Gouveia Dal Pino, E. M., Lazarian, A. 2003. The role of Violent Magnetic Reconnection on the Production of the Large Scale Superluminal Ejections of the Microquasar GRS 1915+105. ArXiv Astrophysics e-prints arXiv:astro-ph/0307054. (preprint version of 2005, A&A, 441, 845-853)
- de Gouveia dal Pino, E. M., Lazarian, A. 2005. Production of the large scale superluminal ejections of the microquasar GRS 1915+105 by violent magnetic reconnection. Astronomy and Astrophysics 441, 845–853.
- Draine, B. T., Lazarian, A. 1998. Electric Dipole Radiation from Spinning Dust Grains. The Astrophysical Journal 508, 157–179.
- Drake, J. F. 2001. Magnetic explosions in space. Nature 410, 525–526.
- Drake, J. F., Swisdak, M., Che, H., Shay, M. A. 2006. Electron acceleration from contracting magnetic islands during reconnection. Nature 443, 553–556.
- Drake, J. F., Opher, M., Swisdak, M., Chamoun, J. N. 2010. A Magnetic Reconnection Mechanism for the Generation of Anomalous

- Cosmic Rays. The Astrophysical Journal 709, 963–974.
- Elmegreen, B. G., Scalo, J. 2004. Interstellar Turbulence I: Observations and Processes. Annual Review of Astronomy and Astrophysics 42, 211–273.
- Fisk, L. A., Gloeckler, G. 2006. The Common Spectrum for Accelerated Ions in the Quiet-Time Solar Wind. The Astrophysical Journal 640, L79–L82.
- Florinski, V., Zank, G. P. 2006. Particle acceleration at a dynamic termination shock. Geophysical Research Letters 33, 15110.
- Fox, D. B., and 35 colleagues 2005. The afterglow of GRB 050709 and the nature of the short-hard γ -ray bursts. Nature 437, 845–850.
- Galama, T. J., and 48 colleagues 1998. An unusual supernova in the error box of the γ -ray burst of 25 April 1998. Nature 395, 670–672.
- Haverkorn, M., Brown, J. C., Gaensler, B. M., McClure-Griffiths, N. M. 2008. The Outer Scale of Turbulence in the Magnetoionized Galactic Interstellar Medium. The Astrophysical Journal 680, 362–370.
- Heraclitus of Ephesus: Fragments: the collected wisdom of Heraclitus, Viking, New York, 2001.
- Huang, Y.-M. and Bhattacharjee, A.: Scaling laws of resistive magnetohydrodynamic reconnection in the high-Lundquist-number, plasmoid-unstable regime, Physics of Plasmas, 17, 062 104—+, doi:10.1063/1.3420208, 2010.
- Kadomtsev, B.: Tokamak Plasma: A Complex Physical System, IOP Publishing, Bristol, 1992.
- Innes, D. E., Inhester, B., Axford, W. I., Wilhelm, K. 1997. Bidirectional plasma jets produced by magnetic reconnection on the Sun. Nature 386, 811–813.
- Jokipii, J. R., Giacalone, J. 1998. The Theory of Anomalous Cosmic Rays. Space Science Reviews 83, 123–136.
- Jokipii, R. 1999. Cosmic Rays in Interstellar Turbulence. Interstellar Turbulence 70.
- Lapenta, G.: Self-Feeding Turbulent Magnetic Reconnection on Macroscopic Scales, Physical Review Letters, 100, 235 001—+, doi:10.1103/PhysRevLett.100.235001, 2008.
- Lazarian, A., Vishniac, E. T. 1999. Reconnection in a Weakly Stochastic Field. The Astrophysical Journal 517, 700–718.
- Lazarian, A., Vishniac, E. T., Cho, J. 2004. Magnetic Field Structure and Stochastic Reconnection in a Partially Ionized Gas. The Astrophysical Journal 603, 180–197.
- Lazarian, A. 2005. Astrophysical Implications of Turbulent Reconnection: from cosmic rays to star formation. Magnetic Fields in the Universe: From Laboratory and Stars to Primordial Structures. 784, 42–53.
- Lazarian, A., Opher, M. 2009. A Model of Acceleration of Anomalous Cosmic Rays by Reconnection in the Heliosheath. The Astrophysical Journal 703, 8–21.
- Loureiro, N. F., Schekochihin, A. A., and Cowley, S. C.: Instability of current sheets and formation of plasmoid chains, Physics of Plasmas, 14, 100 703—+, doi:10.1063/1.2783986, 2007.
- Loureiro, N. F., Uzdensky, D. A., Schekochihin, A. A., Cowley, S. C., and Yousef, T. A.: Turbulent magnetic reconnection in two dimensions, Mon. Not. Royal Astron. Soc., 399, L146–L150, doi:10.1111/j.1745-3933.2009.00742.x, 2009.
- Lovelace, R. V. E. 1976. Dynamo model of double radio sources. Nature 262, 649–652.
- Masuda, S., Kosugi, T., Hara, H., Tsuneta, S., Ogawara, Y. 1994. A

- loop-top hard X-ray source in a compact solar flare as evidence for magnetic reconnection. Nature 371, 495–497.
- Matthaeus, W. H., Lamkin, S. L. 1985. Rapid magnetic reconnection caused by finite amplitude fluctuations. Physics of Fluids 28, 303–307.
- Matthaeus, W. H., Lamkin, S. L. 1986. Turbulent magnetic reconnection. Physics of Fluids 29, 2513–2534.
- McComas, D. J., Schwadron, N. A. 2006. An explanation of the Voyager paradox: Particle acceleration at a blunt termination shock. Geophysical Research Letters 33, 4102.
- McKee, C. F., Ostriker, E. C. 2007. Theory of Star Formation. Annual Review of Astronomy and Astrophysics 45, 565–687.
- Moraal, H., Caballero-Lopez, R. A., McCracken, K. G., McDonald,
 F. B., Mewaldt, R. A., Ptuskin, V., Wiedenbeck, M. E. 2006.
 Cosmic ray energy changes at the termination shock and in the heliosheath. Physics of the Inner Heliosheath 858, 219–225.
- Ng, C. S. and Ragunathan, S.: High Lundquist Number Resistive MHD Simulations of Magnetic Reconnection: Searching for Secondary Island Formation, ArXiv e-prints, 2011.
- Ni, L., Germaschewski, K., Huang, Y.-M., Sullivan, B. P., Yang, H., and Bhattacharjee, A.: Linear plasmoid instability of thin current sheets with shear flow, Physics of Plasmas, 17, 052 109—+, doi: 10.1063/1.3428553, 2010.
- Ossendrijver, M. 2003. The solar dynamo. Astronomy and Astrophysics Review 11, 287–367.
- Parker, E. N. 1957. Sweet's Mechanism for Merging Magnetic Fields in Conducting Fluids. Journal of Geophysical Research 62, 509–520.
- Parker, E. N.: The Solar-Flare Phenomenon and the Theory of Reconnection and Annihiliation of Magnetic Fields., Astrophys. J. Suppl., 8, 177—+, doi:10.1086/190087, 1963.
- Parker, E. N. 1970. The Generation of Magnetic Fields in Astrophysical Bodies. I. The Dynamo Equations. The Astrophysical Journal 162, 665.
- Parker, E. N. 1979. Cosmical magnetic fields: Their origin and their activity. Oxford, Clarendon Press; New York, Oxford University Press, 1979, 858 p. .
- Parker, E. N. 1993. A solar dynamo surface wave at the interface between convection and nonuniform rotation. The Astrophysical Journal 408, 707–719.
- Parnell, C., Haynes, A., and Galsgaard, K.: Recursive Reconnection and Magnetic Skeletons, Astrophys. J., 675, 1656, 2008.
- Petschek, H. E., 1964, Magnetic field annihilation. In: W. H. Hess (Ed.), The Physics of Solar Flares. Proceedings of the AAS-NASA Symposium, 28–30 October, 1963, at the Goddard Space Flight Center, Greenbelt, MD, U.S.A. NASA Special Publication 425
- Priest, E. and Forbes, T.: Magnetic Reconnection: MHD Theory and Applications, Cambridge University Press, Cambridge, 2000.
- Priest, E. R., Forbes, T. G. 2002. The magnetic nature of solar flares. Astronomy and Astrophysics Review 10, 313–377.
- Rutherford, P. H.: Nonlinear growth of the tearing mode, Physics of Fluids, 16, 1903–1908, doi:10.1063/1.1694232, 1973.
- Samtaney, R., Loureiro, N. F., Uzdensky, D. A., Schekochihin, A. A., and Cowley, S. C.: Formation of Plasmoid Chains in Magnetic Reconnection, Physical Review Letters, 103, 105 004—+, doi:10.1103/PhysRevLett.103.105004, 2009.
- Schindler, K.: Physics of Space Plasma Activity, Cambridge Uni-

- versity Press, Cambridge, doi:10.2277/0521858976, 2006.
- Schindler, K. and Birn, J.: Thin current sheets and magnetotail dynamics, J. Geophys. Res., 1042, 25 001–25 010, doi:10.1029/ 1999JA900258, 1999.
- Shay, M. A., Drake, J. F. 1998. The role of electron dissipation on the rate of collisionless magnetic reconnection. Geophysical Research Letters 25, 3759–3762.
- Shibata, K., Tanuma, S. 2001. Plasmoid-induced-reconnection and fractal reconnection. Earth, Planets, and Space 53, 473–482.
- Shimizu, T., Kondo, K., Ugai, M., Shibata, K. 2009. Magnetohydrodynamics Study of Three-Dimensional Fast Magnetic Reconnection for Intermittent Snake-Like Downflows in Solar Flares. The Astrophysical Journal 707, 420–427.
- Skender, M. and Lapenta, G.: On the instability of a quasiequilibrium current sheet and the onset of impulsive bursty reconnection, Physics of Plasmas, 17, 022 905—+, doi:10.1063/1.3299326, 2010.
- Stix, M. 1975. The galactic dynamo. Astronomy and Astrophysics 42, 85–89.
- Sturrock, P. A. 1966. Model of the High-Energy Phase of Solar Flares. Nature 211, 695–697.
- Sweet, P.: The production of high energy particles in solar flares, Il Nuovo Cimento (1955-1965), 8, 188–196, http://dx.doi.org/10. 1007/BF02962520, 10.1007/BF02962520, 1958.
- Sweet, P. A. 1958. The Neutral Point Theory of Solar Flares. Electromagnetic Phenomena in Cosmical Physics 6, 123.
- Uzdensky, D. A., Loureiro, N. F., and Schekochihin, A. A.: Fast Magnetic Reconnection in the Plasmoid-Dominated Regime, Physical Review Letters, 105, 235 002—+, doi:10.1103/ PhysRevLett.105.235002, 2010.
- Yokoyama, T., Shibata, K. 1995. Magnetic reconnection as the origin of X-ray jets and H α surges on the Sun. Nature 375, 42–44.
- Zhang, M. 2006. Acceleration of galactic and anomalous cosmic rays in the heliosheath. Physics of the Inner Heliosheath 858, 226–232.

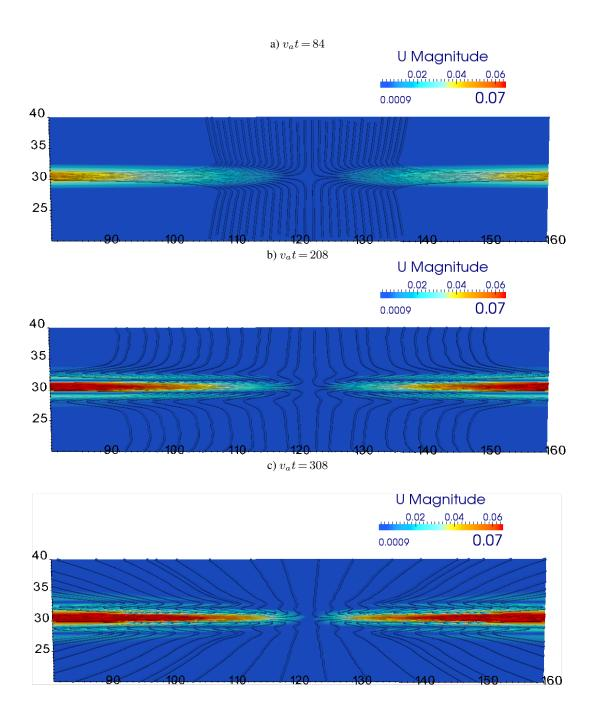


Fig. 5. Early evolution. The flow lines are shown superimposed over a false colour representation of the flow speed. The SP layer first forms and the flow pattern around it changes its nature. Three times are shown. Blow up of the central region, the full box is 240x60.

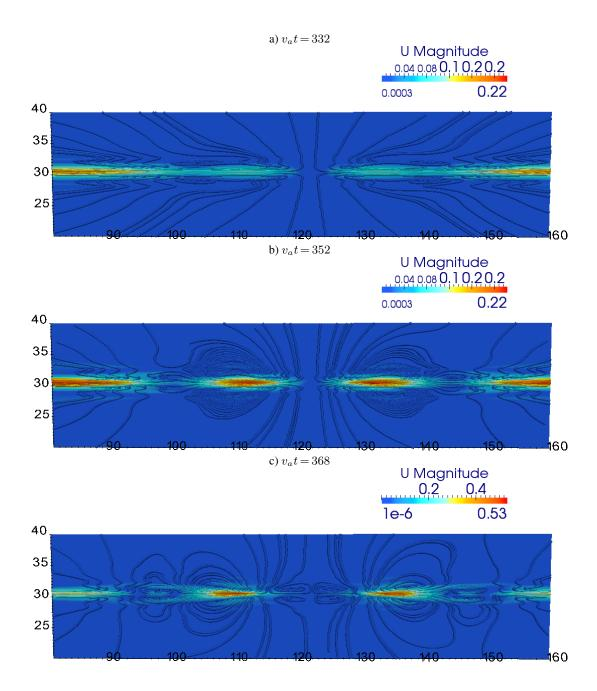


Fig. 6. Later evolution. The flow lines are shown superimposed over a false colour representation of the flow speed. The SP layer is destabilised by the secondary island instability. Three times are shown. The first two have the same color scale, but the third has higher values to avoid saturation. Blow up of the central region, the full box is 240x60.

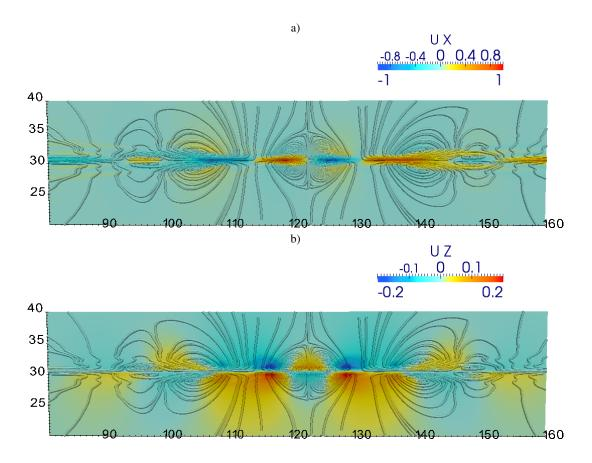


Fig. 7. Flow pattern at time $t/\tau_A=375.5$. The outflow component U_x is shown in panel a and the inflow component z in panel b. Blow up of the central region, the full box is 240x60.

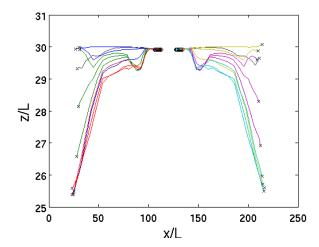


Fig. 8. Trajectory of Lagrangian markers. Miltiple trajectories are shown in different colours. Each trajectory starts at a circle and ends at a cross. The initial positions for the aprticles are equallys paced between $x-L_x=\pm 7L$ and $x-L_x/2=\pm 14L$ on either side from the center of the x axis and at vertical position z/L=29.9167, just a little below the central neutral line.